Microbiology (2005), **151**, 3679–3688 DOI 10.1099/mic.0.28328-0

Surface ultrastructure and elasticity in growing tips and mature regions of *Aspergillus* hyphae describe wall maturation

Hui Ma,[1] Laelie A. Snook,[1] Susan G. W. Kaminskyj[2]† and Tanya E. S. Dahms[1]†

[1]Department of Chemistry and Biochemistry, University of Regina, 3737 Wascana Parkway, Regina, SK, Canada S4S 0A2

[2]Department of Biology, University of Saskatchewan, Saskatoon, SK, Canada S7N 5E2

Correspondence
Tanya E. S. Dahms
tanya.dahms@uregina.ca

Received 7 July 2005
Revised 30 July 2005
Accepted 2 August 2005

This study reports the first direct, high-resolution physical and structural evidence of wall changes during hyphal tip growth, visualized by atomic force microscopy (AFM) in *Aspergillus nidulans*. Images from AFM and cryo-scanning electron microscopy provided comparable information, but AFM was also able to image and physically probe living cells. AFM images showed changes in the surface ultrastructure of *A. nidulans* hyphae, from newly deposited walls at hyphal tips to fully mature walls, as well as additional changes at young branches arising from mature walls. Surface architecture during wall maturation correlated with changes in the relative viscoelasticity (compliance per unit applied force) of walls measured by force spectroscopy (FS) in growing *A. nidulans* hyphae. Growing tips showed greater viscoelasticity than mature walls, despite equal support from turgor. Branch tips had comparable viscoelasticity to hyphal tips, unlike the mature wall from which they grew. FS also revealed differences in surface hydrophilicity between newly deposited and mature walls, with the tips being more hydrophilic. The hydrophilicity of young branch tips was similar to that of hyphal tips, and different from that of mature walls. Taken together, AFM images and FS data suggest that the *A. nidulans* wall matures following deposition at the hyphal tip.

INTRODUCTION

For filamentous fungi, hyphal tip growth is central to all types of invasive disease, and depends on fungal wall properties. After more than a century of research, our understanding of the physiological details of tip growth is considerable, but until this report, dynamic and detailed information about the wall structure of growing tips has been limited by the lack of appropriate technology.

Tip extension is the highly conserved polarized growth pattern characteristic of fungi (Bartnicki-García, 2003; Harold, 2002; Momany, 2002), oomycetes (Meyer *et al.*, 1976), plant pollen tubes (Yang, 1998) and root hairs (Mathur & Hulskamp, 2002). Tip-growing cells are structurally and functionally polarized, so that their growth direction is highly predictable, and polarity is essential for directed movement in all cell types (Small & Kaverina, 2002; Wedlich-Soldner & Li, 2003). Fungal hyphae provide an attractive model for studying tip growth, and the filamentous fungus *Aspergillus nidulans* is especially suitable. The fungal cytoplasm is surrounded by a cell membrane that in turn is encased in a wall, consisting in *Aspergillus* primarily of a carbohydrate matrix, composed of (1→3)- and (1→6)-β-glucans, reinforced by chitin microfibrils (Beckett *et al.*, 1974; Guest & Momany, 2000; Lipke & Ovalle, 1998; Vermeulen & Wessels, 1984, 1986). Internal hydrostatic pressure (turgor), typically several atmospheres [1·4 MPa (Beever & Laracy, 1986)], presses the cell membrane tightly against the wall. Turgor is a non-polarized component of tip-growing cells, since its force is equal in all directions. Turgor can vary dramatically without substantial changes in growth rate, and vice versa, so local regulation of wall and cytoskeletal properties is proposed to influence tip growth rate (Money & Harold, 1992; Money & Hill, 1997). As reviewed by Bartnicki-García (2003), tip growth requires the insertion of new membrane and wall-forming materials (matrix components via exocytosis, and wall fibrils synthesized *in situ* by integral enzymes) at the apex (Bartnicki-García & Lippman, 1972; Bartnicki-García *et al.*, 2000; Gooday, 1994), so the tip wall must be able to accommodate new material during cell growth. Growing tips are protected against rupture from turgor through internal reinforcement

†These authors contributed equally to the written manuscript.

Abbreviations: AFM, atomic force microscopy; CM, complete medium; cryoSEM, scanning electron microscopy of frozen hydrated cells; FS, force spectroscopy; FWHM, full width at half maximum; SEM, scanning electron microscopy.

by actin microfibril arrays that are secured to transmembrane proteins (Kaminskyj & Heath, 1995; Torralba & Heath, 2001). In sum, tip growth in fungal hyphae results from the interplay between localized wall deposition, localized internal cytoskeletal support, a gradient of wall maturation, and turgor that acts evenly along the cell to produce a tubular cell capable of invading nutritive substrates.

Mature *Aspergillus* conidia have a surface hydrophobin rodlet layer (Stringer *et al.*, 1991) that is shed prior to germination. Following germination, cell growth is localized to hyphal tips, so that the distance behind the tip is correlated with the age of the wall. Growing tip walls incorporate new material for cell extension (reviewed by Bartnicki-García, 2003), whereas mature basal walls are fully cross-linked and inextensible (Gooday, 1994). During hyphal-wall maturation, chitin microfibrils are synthesized by enzymes in the cell membrane and are then cross-linked to matrix components (Sietsma & Wessels, 1979, 1981). In *A. nidulans*, the major zone of hyphal expansion is in the apical 3 μm, and approximates to a hemispheric dome (Gierz & Bartnicki-García, 2000). At typical growth rates (0·2–0·5 μm min^{-1}; Kaminskyj & Hamer, 1998), hyphal-wall maturation is probably complete within the apical 6 μm of growth, coincident with the base of the internal actin reinforcement (Fig. 1B in Shi *et al.*, 2004). Branching involves the formation of a new tip, typically from the mature wall, requiring that the branch site be made extensible, likely the result of the localized release of enzymes (Bartnicki-García, 2003; Dynesen & Nielsen, 2003; Harold, 2002; Money & Hill, 1997), some of which have been shown to be endoglucanases (Money & Hill, 1997). Wall 'softness' has also been suggested to contribute to wall extensibility at the apex during tip growth (Bartnicki-García & Lippman, 1972; Gooday, 1994; Money & Harold, 1992).

Growth models described by Wessels (1999) and Bartnicki-García (2003) suggest that wall softness at the tip is necessary for extensibility, although their mechanistic details differ. Until now, evidence for greater extensibility of the tip versus mature regions of the hypha has been circumstantial: mechanical or osmotic insult cause hyphae to burst at or near the tip (Bartnicki-García & Lippman, 1972); growing tips have concentrated cortical actin arrays (Heath, 1990); chemicals that interfere with the actin cytoskeleton or with wall maturation cause tip swelling (Jackson & Heath, 1990); tip-wall biochemistry differs from that of basal walls (Sietsma & Wessels, 1979, 1981; Vermeulen & Wessels, 1984, 1986).

Atomic force microscopy (AFM) can be used in microbiology (Dufrêne, 2004; Firtel & Beveridge, 1995) to image surface detail at the nanometre scale, and to directly address the relationship between the viscoelasticity and extensibility of living tip-growing cells at high resolution by force spectroscopy (FS). Force curves record the deflection of a flexible cantilever as a function of distance when applying force to a specimen through contact with the cantilever-mounted tip, and can be converted to viscoelasticity (force compliance), for example, in specific regions of wall maturation. Theoretical models can then be used to provide quantitative estimates of specimen elasticity (e.g. Young's modulus).

We have used AFM, in combination with techniques such as scanning electron microscopy of frozen hydrated cells (cryoSEM), to examine the surface features of *A. nidulans* hyphae, and FS to probe relative wall rigidity at cell tips, branch junctions and basal regions in growing hyphae, or as a function of tip extension.

METHODS

Biological material and growth conditions. *Aspergillus nidulans* strain A28 (*pabaA6*, *biA1*, *veA1*; www.fgsc.net) was maintained on complete medium (CM) (Kaminskyj, 2001). Strain A28 is morphologically wild-type. Freshly harvested conidia were germinated and grown overnight on a dialysis membrane overlying solid CM, or on coverslips in liquid CM.

Samples for scanning electron microscopy (SEM) and AFM consisted of hyphae growing on the surface of a substrate, either under a coverslip submerged in liquid CM for fixed samples, or on dialysis tubing overlying solid CM for live and cryoSEM samples. Cell morphology and growth rate was wild-type under these constrained conditions, except that the hyphae grew along the substrate surface rather than in three dimensions.

Fresh spores were harvested from conidiating cultures, typically 2–3 days following inoculation. For AFM studies of conidia, glass coverslips were silanized (2 % octadecyltrichlorosilane/hexane), rinsed (hexane), air-dried overnight and touched to a conidiating culture so that a layer of conidia adhered. Non-adherent spores were removed with compressed air before imaging by AFM.

Preparation of fixed cells for AFM. Hyphae grown overnight on dialysis tubing overlying CM agar were fixed by inverting the Petri dish over (not in) drops (200 μl) of OsO_4 (4 % aqueous) placed in the lids. OsO_4 is highly volatile, so cells were vapour-fixed from a source about 3 mm distant. Cells were fixed [at least 2 h at room temperature (RT)], until the underlying agar was dark from Os accumulation. Pieces of dialysis tubing with fixed cells were frozen by plunging into cold anhydrous acetone (60 ml, −80 °C), dehydrated (at least 4 h at −80 °C), warmed slowly to avoid condensation (2 h at −20 °C, 2 h at 4 °C, 2 h at RT), and critical-point dried. For the aforementioned procedure, the acetone is exchanged for liquid CO_2 (in a pressure chamber), which is taken through a phase transition to gas as the temperature is raised through the critical point, circumventing surface-tension artifacts. Dried samples were mounted on aluminium stubs (for SEM) or glass coverslips (for AFM) with double-sided tape, and gold sputter coated. Some AFM samples were imaged without gold coating. Images of fixed, coated and uncoated AFM samples were comparable (data not shown), but gold coating facilitated fast-contact-mode imaging. Some SEM samples were later imaged by AFM for direct comparison.

Preparation for cryoSEM. Cultures were grown (16 h) on dialysis tubing overlying CM agar, frozen in nitrogen slush (−196 °C) and transferred to the SEM specimen chamber (−80 °C). Surface water was removed by sublimation (10 min, −60 °C). Samples were gold coated and examined at −80 °C using a 1630C field emission

scanning electron microscope (JEOL USA) equipped with digital image capture (Department of Earth Sciences, University of Alberta). Images were processed for optimal contrast.

AFM and FS of live cells. Samples were grown overnight on dialysis tubing overlying CM agar. Subsequently, cells were hydrated and nourished by supplying CM liquid to a paper wick under the dialysis tubing (i.e. cells were not immersed), which was mounted on mica and secured with tape. Samples were transferred to the AFM stage and incubated (2 h, 28 °C) to allow hyphae to re-establish growing tips after handling. AFM images were collected in contact mode at high resolution (1000 × 1000 lines). Hyphal growth rate was estimated by stationary line scanning, beginning as a hyphal tip grew past the scan line and continuing until the hyphal width stabilized. Hyphal width reached 2·9 ± 0·4 μm (n = 20), similar to the mean width at the septa of A28 hyphae grown at 28 °C (Kaminskyj & Hamer, 1998), at approximately 3 μm behind the tip.

AFM imaging conditions. An Explorer atomic force microscope (Veeco) with a dry scanner (Veeco, 10 μm in z and 100 × 100 μm in x and y, model 5460-00) was used for imaging and FS. The atomic force microscope was suspended by bungee cords on an iron plate for vibrational isolation, in a wooden cabinet insulated with Sonex foam for sound isolation, which was seated on an optical table (Coherent Ealing Optics) mounted on I-2000 pneumatic isolators (Newport). Hyphae were visually selected using a CCD camera (200 × magnification), followed by imaging at low resolution (200 × 200 lines per scan). Data were collected from high-resolution images (1000 × 1000 lines per scan, scan rate = 1 Hz) of fixed cells using Si_3N_4 probe tips (Veeco model #1520-00, k = 0·032 nN nm^{-1}, nominal resonance v = 17 kHz).

For living cells, 'intermittent contact' and 'non-contact' modes were sometimes used to collect images with Si probe tips (Veeco model #1650-00, k = 2 nN nm^{-1}, v = 230–280 kHz) to prevent samples from sticking to the probe during imaging. For images larger than 5 × 5 μm, a ¼ Hz scan rate was used to avoid dislodging the hyphae. Images smaller than 5 × 5 μm were acquired at ½–¾ Hz. All images represent typical results.

The varying geometry and characteristics of AFM probes may cause image distortion and overestimation of the lateral size of small features (x and y). Therefore, to minimize experimental error, we tested all AFM probes (Xu & Arnsdorf, 1994) using colloidal gold particles (0·01 % $HAuCl_4$ in 0·02 % NaN_3) with a radius of 5 nm, showing that our tips were capable of resolving these spheres within the experimental error [full width at half maximum (FWHM) = 5·3 nm ± 0·4 nm, n = 20). To test whether we could resolve fine features (10 nm) on a topographically complicated surface, we imaged dry-harvested conidia, which have been studied elsewhere at high resolution with SEM (Beever & Dempsey, 1978).

Images were processed using horizontal levelling, with the maximal height adjusted for optimum contrast (SPMLab version 6.0 software, Veeco). Since images of the surface result from a convolution of the shapes of the AFM probe and surface features, widths were measured at the FWHM of the peak height, and both widths and heights were measured manually using the line measurement option. In some cases, images have been presented enlarged for clarity. Data are presented as mean ± standard deviation. Differences in the mean subunit sizes in apical, subapical and branch-point junction regions were tested by a one-way ANOVA using InStat 3 (GraphPad).

Force spectroscopy (FS). For FS, the AF microscope was equipped with hydrophilic Si_4N_3 probe tips. The interaction between the AFM probe and the sample was tracked by cantilever deflection (Z_c) as a function of the piezo elongation (Z_p) during probe approach and retraction. For soft materials, meaningful FS comparisons depend on the velocity of the surface approach. The approach velocity (10 μm s^{-1}) was kept constant to facilitate the comparison of relative viscoelasticity and adhesion forces measured at different regions of the sample. Repeated measurements of individual sites on mature walls gave consistent values and images obtained before and after FS were unchanged (data not shown), indicating that the walls were not damaged during data collection. FS measurements (4–6 per area on each hypha) were collected from the hyphal wall in the apical expansion zone (1 μm steps), and from the mature wall 20 and 40 μm from the tip. FS data were also collected at tips of branches about 2 μm long, at hypha-to-branch junctions, and on the mature wall of the subtending hypha.

During FS, the magnitude of AFM-probe deflection per unit of applied force is measured as the probe approaches and retracts from the sample. Probe responses during the approach–retract cycle, summarized as force curves, can be used to measure the unit force required to indent a surface a given distance. The last portion of the approach cycle (Fig. 6B, line b–c) and the first part of the retraction cycle (Fig. 6B, line c–d) can be used to examine the relative rigidity of the surface. For a hard surface such as glass, the slope of the line b–c during the approach cycle will be identical to that (c–d) during retraction (Fig. 6B insert). In contrast, sample deformation will appear as a difference between the slopes b–c and c–d (Fig. 6B). Adhesion values are measured from the last segment of the retraction cycle (Fig. 6B, line e–f), and if there is chemical attraction between the sample and the AFM probe, segment e–f will be a measure of its intensity.

FS data were initially plotted as Z_c (nA) versus Z_p (nm), and then converted to force (nN) versus distance (nm) curves using the spring constant of the cantilever. The slope of the line (N m^{-1}) was then used to determine the spring constant k_w of the cell wall, used for the subsequent determination of Young's modulus according to the equation (Zhao *et al.*, 2005):

$$E = 0{\cdot}80\frac{k_w}{h}\left(\frac{R}{h}\right)^{1{\cdot}5}$$

where E is the cell wall elastic modulus, R is the hyphal radius measured by AFM, and h is the thickness of the cell wall measured by transmission electron microscopy (Kaminskyj & Boire, 2004). Differences in the cell wall elastic modulus at apical, subapical and branch-point junction regions were assessed by one-way ANOVA (InStat 3, GraphPad). Propagated standard errors were calculated for Young's moduli at the tip and mature regions, and a Student's t test (two-tailed) was used to assess significant difference (Prism, GraphPad).

Since the aim was to report relative changes in elasticity along hyphae, a single AFM cantilever (spring constant k = 0·032 nN nm^{-1}, Veeco) and tip were used for all FS measurements. The force exerted by the piezo on the cantilever was 0·125 nN for each nA of deflection.

RESULTS

By 16 h after inoculation, *A. nidulans* germlings were at least 100 μm long, and had produced at least one long hypha and one lateral branch from near its base (data not shown). Both septum insertion and branching were observed where the hyphal wall had matured.

Surface morphology

Fig. 1 shows cryoSEM (Fig. 1A) and AFM (Fig. 1B) images of fixed mature hyphal wall surfaces of *A. nidulans*, each taken ⩾40 μm behind the tip. Both imaging methods show rounded features, the diameter (25 ± 6 nm, n = 60, range

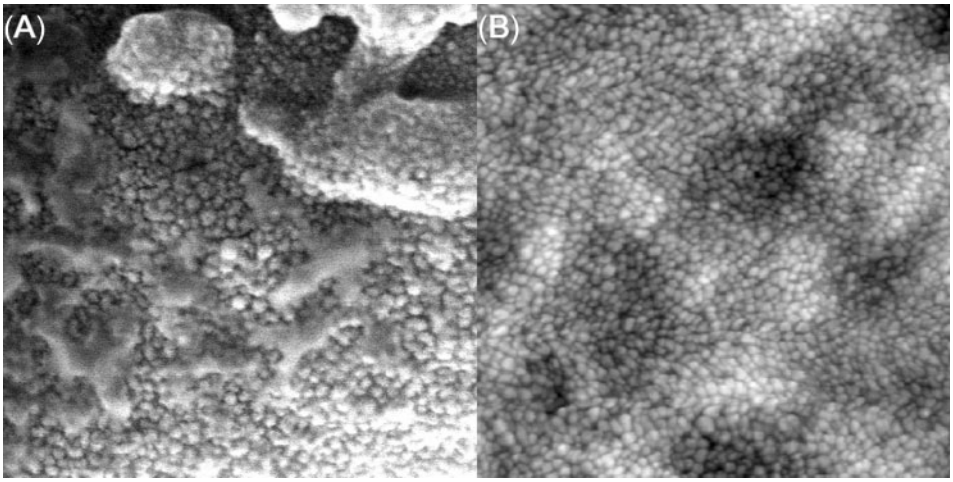

Fig. 1. Images of *Aspergillus nidulans* mature hyphal walls ($\geqslant$20 μm from apex). Walls were imaged using (A) cryoSEM and (B) AFM for fixed samples, showing rounded surface features 25 ± 6 nm in diameter. The cryoSEM specimen in (A) retained a small amount of surface water following sublimation, which appears as raised amorphous regions, whereas (B) had been critical-point dried prior to imaging. Each image is 1·5 × 1·5 μm.

15–37 nm) of which was measured from AFM images. Critical-point drying maintains three-dimensional structures far better than freeze-drying or air drying (data not shown), and was therefore used for all specimens except those used for cryoSEM and AFM of live samples. There was no qualitative or quantitative difference between AFM images of fixed hyphae with or without gold coating (data not shown). Fig. 1(A) also shows small areas in the cryoSEM image in which vitreous water had not been removed by sublimation before gold coating. As yet we have little evidence for the shape and/or packing of the surface features within the wall. We used SEM and AFM to image the hyphal wall surface, so our use of 'rounded' (and later 'ellipsoid') refers only to the surface appearance of the features.

The surface of hyphal walls viewed with cryoSEM is distinctly different from the rodlets characteristic of conidial surfaces (Beever & Dempsey, 1978; Stringer *et al.*, 1991), which are 10 ± 2 nm wide (n = 60) and more than 100 nm long. AFM was able to image these details on topographically complex spore surfaces (Fig. 2).

We used AFM to examine whether or not the expansion zone at the hyphal tip would appear different from the mature hypha, given the biochemical changes that accompany fungal wall maturation. AFM images of the wall within the first 3 μm of the tip of fixed *A. nidulans* hyphae (Fig. 3A) showed ellipsoid features (short axis 22–35 nm, long axis 28–70 nm, n = 60), with the long axis transverse to the growth direction. Wall surface features in the expansion region were larger and more variable in size than those of mature walls (cf. Figs 4A and 3B, C). Features in mature walls 20 μm and 40 μm from the tip were similar in appearance and average diameter.

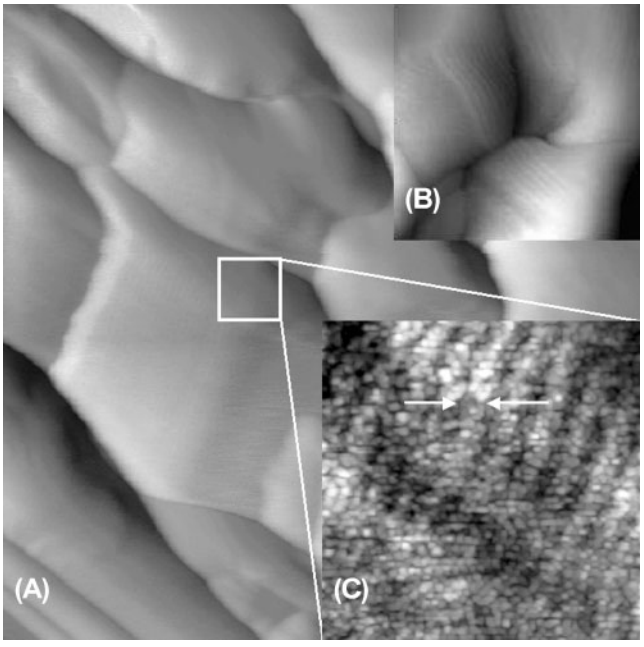

Fig. 2. Lateral force image (1·5 × 1·5 μm) of an *Aspergillus nidulans* conidium. The sample was transferred from the dry surface of a sporulating culture onto a silanized glass surface and imaged by AFM in contact mode (A). The top right inset (0·4 × 0·4 μm) is a topography image (B) and the bottom right inset (0·15 × 0·15 μm) shows the 10 nm wide rodlets (between arrows), characteristic of the structures formed by monomers of a hydrophobic protein (hydrophobin) that coats fungal spores and other aerial structures (C), and that are distinctly different from the surface features of the hyphal walls grown in moist environments (cf. Figs 2 and 4).

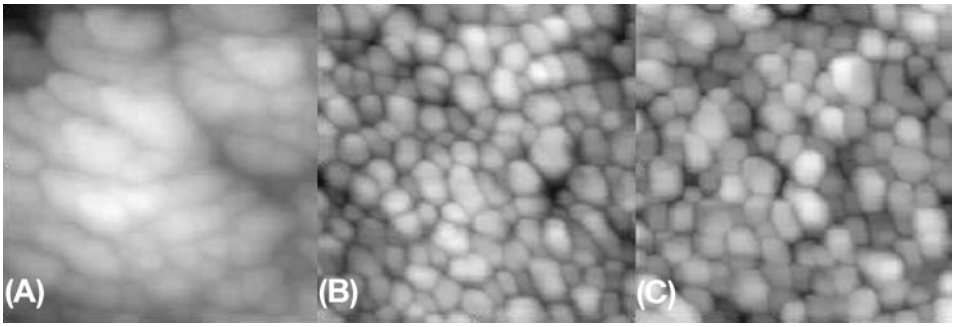

Fig. 3. *Aspergillus nidulans* hypha fixed with osmium tetroxide vapour, substituted and dried at critical point, and imaged by AFM in contact mode, showing wall surfaces. Images (0·4 × 0·4 μm) represent the tip (A) and mature regions, 20 μm (B) and 40 μm (C) from the tip. Surface-feature dimensions and statistical analyses are reported within the Results.

The surfaces of fixed hyphae were imaged by AFM (Fig. 4) for comparison with living cells (Figs 2 and 3B, C). Surface undulations in fixed hyphae ($w \sim 290$ nm, $h \sim 275$ nm; Fig. 1) were also observed on live hyphae (Fig. 4); their provenance and significance are uncertain, and might be the result of different phenomena in each case. We resolved surface features (Fig. 4B) in lateral force images of live hyphae similar in size and shape to those from fixed hyphae, but some were significantly larger than those in fixed or frozen samples and had poorly defined topographic features. The image shown in Fig. 4(B) is the surface of a living hyphal wall, at the highest resolution currently achieved. We assessed the possibility of permanent damage to living surfaces by repeated AFM scans over selected areas, finding that there was no difference between the first and last scan in each set (data not shown).

The surface features at young branch tips were similar in size and shape to those at hyphal tips (data not shown), but larger, ellipsoid, and different from those of mature walls. Surface packing at branch points (Fig. 5A) suggested a mixture of mature wall features intercalated with newly deposited ones (Fig. 5B).

Wall rigidity and surface chemistry

Having developed a method to image living hyphae without damage at relatively high resolution, we were able to examine the properties of living hyphae using FS. Initial FS studies on dialysis tubing overlying glass showed that this surface was almost as rigid as the glass itself. Subsequent FS measurements on living hyphae showed that cells were significantly more viscoelastic than the substrates on which they were

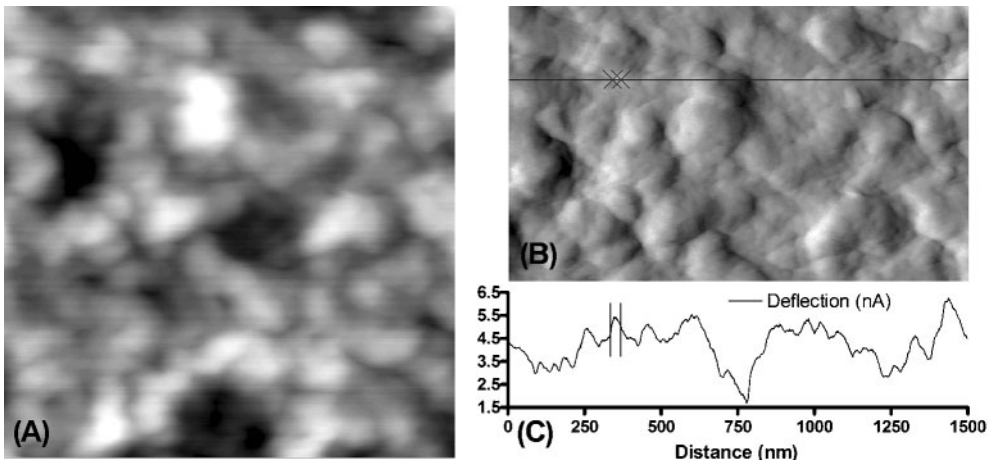

Fig. 4. AFM images (1·5 × 1·5 μm) of the wall surface for a living *Aspergillus nidulans* hypha, in a mature region 40 μm behind a growing tip. Topography (A) and lateral force (B) images show the surface of the living cell wall, for which feature (B) dimensions are of the same order of magnitude [(C), the feature between parallel vertical lines is approximately 26 nm] as those observed in fixed hyphae. The size and shape of the features in the topography images likely represent deformation and/or hyphal movement during contact-mode imaging with the atomic force microscope.

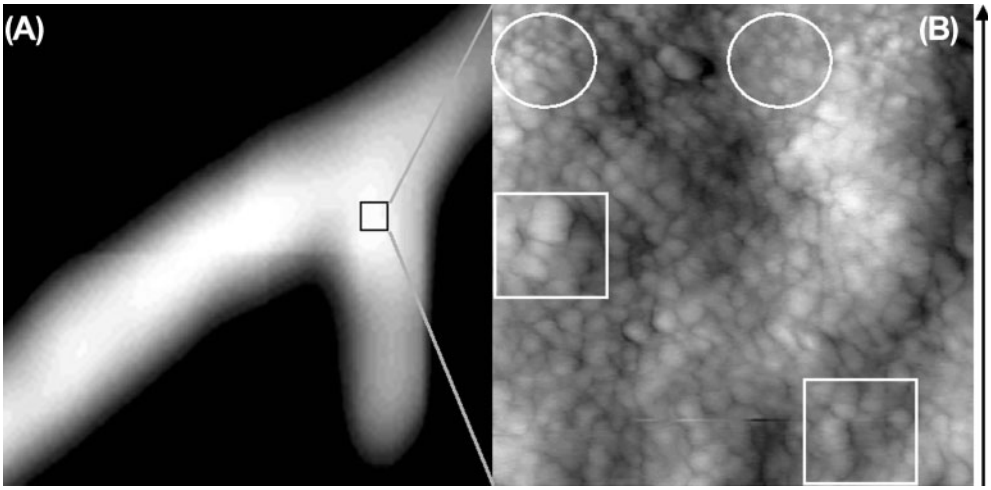

Fig. 5. AFM images of an *Aspergillus nidulans* branch junction from a fixed hypha. The new branch, only the base of which is shown in image (B) ($0{\cdot}8 \times 0{\cdot}8$ μm), is 4 μm in length. (B) The wall at the branch point junction has a wide range of feature sizes and an irregular surface. Larger (squares) and smaller (circles) features are highlighted, and the vertical arrow (at the right of the figure) represents the image orientation starting from the apex towards the subtending mature wall.

growing. The relative rigidity of growing tips, mature hyphae and branch-point junctions (Fig. 6C) was quantified as the slope of the line b–c shown on the force–distance curve (Fig. 6B) during the approach cycle. The AFM image in Fig. 6(A) shows regions of a representative, living *A. nidulans* hypha that was examined by FS. Growth rates for hyphae in these experiments were approximately 250 nm min^{-1}, so tip growth during each FS measurement was no more than 500 nm. Spring constants associated with the cell wall of hyphal tips are reported as relative rigidity (pN nm^{-1}). Growing hyphal tips were significantly less rigid (more viscoelastic) than mature regions (Fig. 6C), i.e. growing tips were indented a greater distance by the same applied force. Unexpectedly, growing hyphal tip walls also showed greater adhesion to the hydrophilic AFM probe (Fig. 6D) than the mature walls. As with hyphal tips, young branches showed a gradient of adhesion to the AFM probe, with the apical wall being the most adhesive. There was no difference in viscoelasticity ($P > 0{\cdot}05$) in regions of the hyphal wall 3, 20 and 40 μm from the apex (Fig. 6C). A gradient of both viscoelasticity (Fig. 6C) and adhesion (Fig. 6D) was observed from the apex of a hypha to 3 μm back from the apex for each 1 μm step. Similarly, FS data from a young branch (Figs 6C, D) show that the branch tip is the least rigid, the mature wall of the subtending hypha is most rigid and the junction between the branch and hypha is intermediate in rigidity.

DISCUSSION

Fungal hyphae grow by apical extension, whereby wall matrix material is deposited at the tip along with wall fibril-synthesizing enzymes that participate in generating a relatively rigid wall a few micrometres behind the apex. Despite intense interest and ongoing efforts by many research groups, our understanding of the dynamics of tip growth has been largely inferential, based on the analysis of fixed specimens, biochemical preparations and genetic mutants. Here we show that AFM imaging of growing hyphae is possible, that AFM provides data similar to cryoSEM, and that changes between apical and mature walls support existing models of tip growth (reviewed by Bartnicki-García, 2003).

Samples for cryoSEM are rapidly frozen and remain at or below $-60\,^{\circ}C$ during subsequent preparation and imaging, making cryoSEM the 'gold standard' for preserving ultrastructural information (Howard & O'Donnell, 1987). However, SEM must infer that specific cells were alive at the moment they were frozen, whereas AFM can image cells known to be growing. In addition to imaging, FS can be applied to sample the cell wall properties on different regions of growing hyphae. Our high-resolution AFM images of the mature wall surfaces of fixed, dry hyphae are quantitatively similar to those from our best high-resolution cryoSEM, which gives us confidence that the differences reported by AFM of growing versus mature wall surfaces are accurate, consistent with the differences between hyphal and spore wall surfaces. Like SEM, AFM images of fixed (and fixed/gold-coated) hyphae produce high-lateral-resolution surface structural data. The manner in which an AFM image is acquired (essentially by touch) gives AFM better depth resolution than SEM, whereas SEM images have better depth of focus and field of view.

The hyphal wall surfaces in apical and mature regions are both composed of regular protrusions, but there are clear differences between their size, shape and packing for newly deposited and mature walls, consistent with models

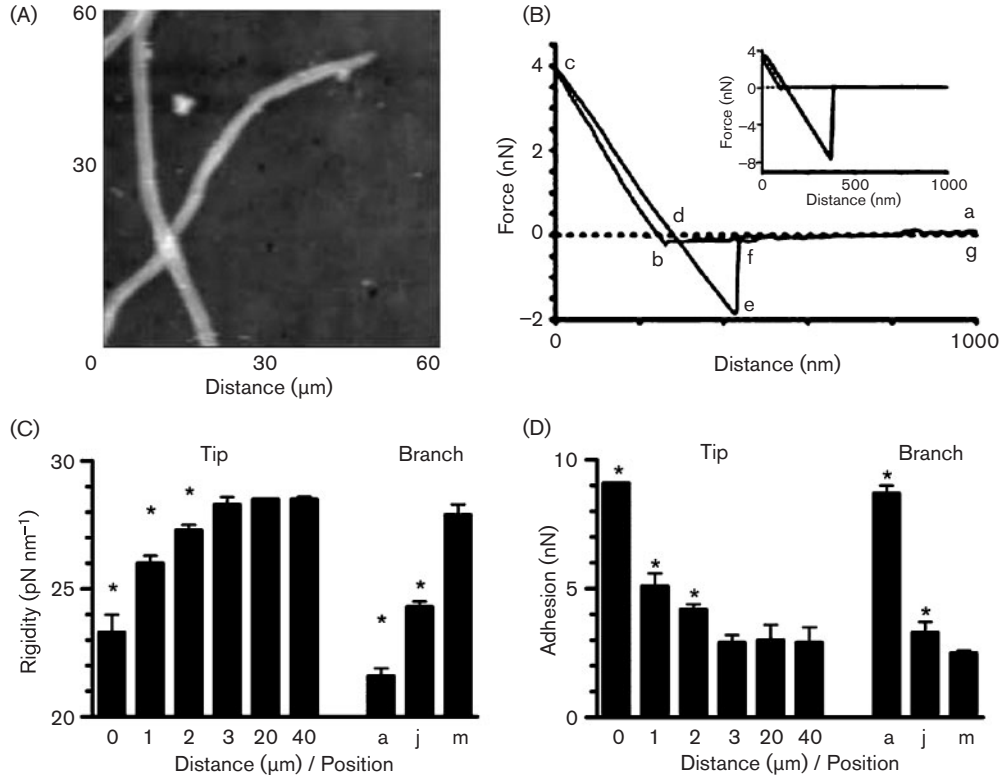

Fig. 6. Force spectroscopy of growing *Aspergillus nidulans* hyphae. (A) AFM image of a representative live hypha used to locate analysis sites at different distances from the tip, for which data are summarized in (C, D). (B) Representative force–distance curve for a mature hyphal wall region shown in (A), together with that of mica (inset). (C) Relative rigidity for growing hyphae and branches formed from mature walls measured behind the apex (0, 1, 2, 3, 20 and 40 μm), at branch tips (a), junctions (j) and the base mature wall (m). A mean value, from six measurements each of the apices of two different live hyphae ($\pm 1{\cdot}1$ pN nm^{-1}), is reported for the tip. (D) Tip–sample adhesion for a growing hypha and branches formed from mature walls measured behind the apex (0, 1, 2, 3, 20 and 40 μm), at branch tips (a), junctions (j), and the base mature wall (m). Error bars (C, D) represent standard deviation, with * indicating a significant difference in rigidity or adhesion compared to mean mature wall values ($P<0{\cdot}001$). Reported are mean values $\pm 0{\cdot}0$–$0{\cdot}8$ pN nm^{-1} (relative rigidity) and $\pm 0{\cdot}1$–$0{\cdot}9$ nN (relative adhesion) from four to six measurements in localized areas (within 0·1 μm) of the different hyphal regions.

suggesting that wall maturation follows deposition (Sietsma & Wessels, 1979, 1981; Vermeulen & Wessels, 1984) and that hyphal wall remodelling can expose or mask epitopes (Momany *et al.*, 2004). The compact, rounded features on the surface of mature walls appear to develop from the rearrangement within and/or lateral packing of the larger ellipsoid features found at hyphal tips. The hyphal-wall surface does not change appreciably between 20 and 40 μm from the tip, and therefore maturation appears to be complete at or before the 20 μm mark.

The width of the rounded features ($\sim$25 nm) is comparable to that of the macromolecular triple helix (triplex) of fungal (1→3)-β-D-glucan derivatives (e.g. scleroglucan: $18 \pm 2{\cdot}5$ nm) that have been characterized *in situ* by electron microscopy and AFM (Stokke *et al.*, 2001). Since the hyphal wall of *A. nidulans* includes glucan polymers (e.g. Guest & Momany, 2000), we speculate that the features on the surface of mature walls could be glucans extending from the cell wall matrix [consistent with the orthogonal expansion pattern of hyphal growth proposed by Bartnicki-García and colleagues (Bartnicki-García *et al.*, 2000; Gierz & Bartnicki-García, 2000)] and/or glycoproteins (Lipke & Ovalle, 1998. The difference in subunit appearance at growing tips compared to mature regions suggests that the wall at the apex could have different mechanical properties, but images alone do not provide evidence for relative rigidity.

This is the first report of using AFM to image growing fungal hyphae. AFM has been used elsewhere to image the surface of live cells at relatively high resolution (Ahimou *et al.*, 2003; Bushell *et al.*, 1999; Cho *et al.*, 2002; Gebeshuber *et al.*, 2003, 2004; Ricci & Grattarola, 1994; Schneider *et al.*, 1997; van der Mei *et al.*, 2000; Yang & Shao, 1995), despite the difficulty in some cases of supporting cell growth during examination. Dufrêne and coworkers (Ahimou *et al.*, 2003) have examined the surface structure of living yeast cells and fungal conidia

in liquid medium (Dufrêne, 2000), but have not yet extended the work to hyphae. Wall undulations were visible for both fixed and live hyphae, with similar size and frequency. Topography images of surface features in living hyphae are not entirely consistent with those in chemically fixed cells. The discrepancy between AFM images of fixed and live hyphae likely results from the reversible deformation of the hyphal wall features in contact with the tip as a result of pressure from the AFM cantilever (Yang & Shao, 1995) and/or subtle movements of the hypha during scanning. These differences could be compounded by cell growth ($\sim$250 nm min^{-1}) at the tip and by the mobility of living hyphal cells that could not be secured firmly to the substrate, since only conidia adhere to dialysis tubing. Nonetheless, the general rounded shape of the surface features and undulations observed in live *A. nidulans* are both consistent with those obtained with AFM for fixed, mature hyphal walls, and are distinctly different from the parallel linear arrangements of the hydrophobin rodlets on spore surfaces. The lateral force image represents high-resolution data for the surface of living hyphal cells that were growing during data capture. The features observed on the surfaces of fixed cells, possibly glycoproteins or glucans (Lipke & Ovalle, 1998; Zhao *et al.*, 2005), can be resolved *in vivo*. We expect in the future to be able to extend this work to examine the dynamics of wall maturation and changes during branch formation, as well as the surface chemistry of specific surface regions, using a variety of chemically modified AFM tips and near-field scanning optical microscopy.

Measurements of hyphal rigidity are most relevant for growing hyphae, which were imaged by AFM and then analysed using FS, showing that walls were less rigid in regions of active extension (hyphal and branch apices) than in mature regions. Consistent with this finding, preliminary FS experiments, in which we were unable to demonstrate hyphal growth, showed no difference between the rigidity of tips and mature walls. Hyphal rigidity will be the sum of contributions from 1) wall elasticity and thickness, 2) internal reinforcement from the cytoskeleton, 3) internal support from turgor, and 4) radius of curvature. Turgor pressure will be evenly distributed along the hypha, while actin is concentrated in the apical 6 μm of the *A. nidulans* tip (Shi *et al.*, 2004), where it is thought to support the extending region. There are only minor differences in thickness between apical (44 ± 3 nm) and mature (48 ± 4 nm) hyphal walls (Kaminskyj & Boire, 2004), too small to explain the almost twofold difference in rigidity that we observe between the two areas of the cell wall. Therefore, differences observed in hyphal rigidity can be attributed to cell wall elasticity (Zhao *et al.*, 2005) and the radius of hyphal curvature.

Arnoldi *et al.* (2000) developed theoretical and experimental models to determine turgor pressure in the Gram-negative bacterium *Magnetospirillum gryphiswaldense* using FS, but the peptidoglycan walls of Gram-negative bacteria are thinner (3–8 nm) than the glucan/chitin walls of *A. nidulans* ($\sim$46 nm; Kaminskyj & Boire, 2004). Nonetheless, applying their model to *A. nidulans* hyphae, using estimates for Young's modulus ($\sim$110 MPa; Zhao *et al.*, 2005), turgor pressure ($\sim$1·4 MPa; Beever & Laracy, 1986) and hyphal width (3 μm), reveals a tension-dominated mode, as expected. According to shell theory (Landau & Lifshitz, 1959) the viscoelasticity of the hypha should vary with its radius of curvature. Therefore, it is still important to demonstrate that the changes in rigidity observed from the growing apex to the mature wall are not solely a function of radius of curvature. *Aspergillus* hyphal tips are approximately parabolic in shape (Gierz & Bartnicki-García, 2000), so that their radius of curvature will be directly proportional to hyphal diameter. If viscoelasticity varies solely with hyphal curvature, we would expect a linear relationship between our rigidity and hyphal diameter measurements, but we find a non-linear relationship (data not shown), implying a significant contribution from cell wall elasticity.

Touhami *et al.* (2003) used force mapping and simple Hertzian models to derive Young's moduli for yeast bud scars and cell surfaces. Their model is valid for elastic surfaces for which adhesion forces are negligible, and is therefore not applicable to hyphae, for which adhesive properties vary from tip to mature wall. Alternatively, Yao *et al.* (1999) isolated cell walls to quantify their viscoelasticity, but this type of analysis, while important, is not relevant for describing dynamic maturation processes in live cells, nor is there a simple way to extract sufficient cell wall material specifically from hyphal tips. A recent study (Zhao *et al.*, 2005) derived Young's moduli for azide-treated (dead), dried, rehydrated hyphae from a theoretical model that relates force measurements directly to wall elasticity. Using their model, we estimate the Young's modulus of the mature wall to be 115 ± 31 MPa, significantly different ($P<0{\cdot}01$) than that of the tip, 75 ± 27 MPa.

Branches were examined for localized changes in wall surface structure and viscoelasticity. Hyphal branching requires that the mature wall be altered to permit extension of the new tip (Bartnicki-García, 2003; Harold, 2002), for which there is experimental evidence in oomycetes (Money & Hill, 1997), and there are also candidate genes for endoglucanases in the *A. nidulans* and *Aspergillus fumigatus* genomes. Consistent with this, the wall structure at branch points was different from that of the subtending mature wall and the tip. Regardless of the mechanism for altering the wall structure, the walls of a growing hyphal tip and of a newly formed branch are expected to be less rigid than a mature wall, which is supported by our FS data. If differences in wall surface structure are related to wall maturation, we might also expect to find lower rigidity at a newly forming branch tip than at the subtending mature wall, and again we find these differences. The rigidity of branch tips was comparable to that of the primary hyphal tip ($P>0{\cdot}05$), as expected, whereas FS values for the subtending mature wall are comparable to other mature wall regions (3–40 μm from the tip). Furthermore, the branch-point junction is much closer in curvature to the subtending mature wall, yet its

rigidity is substantially different, supporting the idea that changes in rigidity at hyphal tips cannot simply be explained by curvature or wall thickness.

The change in hydrophilicity of the hyphal surface as a function of growth, maturation and branching mirrored hyphal viscoelasticity. These results indicate that the wall surface is altered during maturation, by rearrangement and/or through the addition of materials. Capillary forces are generally thought to be responsible for drawing the AFM tip into contact with the sample (point b, Fig. 6B), but as shown here, their magnitude does not overwhelm differences in the hydrophilicity of the wall regions. The adhesive forces measured by FS are the sum of the capillary force F_c, due to Laplace pressure from the water meniscus that forms between the AFM tip and the sample, and the direct adhesion between the two surfaces once in contact. Capillary effects should be relatively uniform along the hypha, whereas the cell wall structure changes with wall maturation, affecting the relative adhesive properties between the cell wall and the AFM tip. By 3 μm behind the tip, hyphal surface subunit diameter, hyphal wall viscoelasticity and surface hydrophilicity were similar to those of mature walls, suggesting that under these growth conditions, the surface of the hyphal wall has 'matured' within approximately 12 min.

Our main findings show that *A. nidulans* hyphae have significant surface-structure and viscoelasticity differences between actively growing tips, branch junctions and mature walls. As the wall matures, the surface-feature size and packing changes, which correlates with hyphal viscoelasticity and surface chemistry, in keeping with previously described biochemical changes. These results are consistent with cross-linking during maturation and structural reorganization at branch points. Locating precise regions of living hyphae with AFM presented the opportunity to measure the relative stiffness of these regions by FS. Hyphal tips and branch points were significantly less rigid than the mature wall at least 3 μm behind the hyphal apex. Together, this is the first direct evidence for localized cell wall changes during hyphal tip growth, and demonstrates the power of combining AFM with FS for live specimens. We have shown a structure–function relationship for *A. nidulans* hyphal walls that corresponds mechanistically with models of tip growth.

ACKNOWLEDGEMENTS

We thank Melissa Boire (University of Saskatchewan), George Braybrook (University of Alberta) for technical support, and Dr C. Tian for preliminary FS data of non-growing hyphae. T. E. S. D. thanks Drs David Cramb, Linda Johnston, Gopalan Selvaraj and Gerry Wright for comments on the manuscript. T. E. S. D. and S. G. W. K. acknowledge support from the Natural Sciences and Engineering Research Council of Canada (NSERC), the Canadian Foundation for Innovation (CFI) and the Saskatchewan Health Research Foundation (SHRF, formerly HSURC). L. A. S. and H. M. were partially supported by University of Regina scholarships.

REFERENCES

Ahimou, F., Touhami, A. & Dufrêne, Y. F. (2003). Real-time imaging of the surface topography of living yeast cells by atomic force microscopy. *Yeast* **20**, 25–30.

Arnoldi, M., Fritz, M., Bäuerlein, E., Radmacher, M., Sackmann, E. & Boulbitch, A. (2000). Bacterial turgor pressure can be measured by atomic force microscopy. *Phys Rev E* **62**, 1034–1044.

Bartnicki-García, S. (2003). Hyphal tip growth: outstanding questions. In *Molecular Biology of Fungal Development*, pp. 29–58. Edited by H. D. Osiewacz. New York: Marcel Dekker.

Bartnicki-García, S. & Lippman, E. (1972). The bursting tendency of hyphal tips of fungi: presumptive evidence for a delicate balance between wall synthesis and wall lysis in apical growth. *J Gen Microbiol* **73**, 487–500.

Bartnicki-García, S., Bracker, C. E., Gierz, G., Lopez-Franco, R. & Lu, H. (2000). Mapping the growth of fungal hyphae: orthogonal cell wall expansion during tip growth and the role of turgor. *Biophys J* **79**, 2382–2390.

Beckett, A., Heath, I. B. & McLaughlin, D. J. (1974). *An Atlas of Fungal Ultrastructure*. London: Longman.

Beever, R. E. & Dempsey, G. P. (1978). Function of rodlets on the surface of fungal spores. *Nature* **272**, 608–610.

Beever, R. E. & Laracy, E. P. (1986). Osmotic adjustment in the filamentous fungus *Aspergillus nidulans*. *J Bacteriol* **168**, 1358–1365.

Bushell, G. R., Cahill, C., Clarke, F. M., Gibson, C. T., Myhra, S. & Watson, G. S. (1999). Imaging and force-distance analysis of human fibroblasts in vitro by atomic force microscopy. *Cytometry* **36**, 254–264.

Cho, S. J., Quinn, A. S., Stromer, M. H., Dash, S., Cho, J., Taatjes, D. J. & Jena, B. P. (2002). Structure and dynamics of the fusion pore in live cells. *Cell Biol Int* **26**, 35–42.

Dufrêne, Y. F. (2000). Direct characterization of the physicochemical properties of fungal spores using functionalized AFM probes. *Biophys J* **78**, 3286–3291.

Dufrêne, Y. F. (2004). Using nanotechniques to explore microbial surfaces. *Nat Rev Microbiol* **2**, 451–460.

Dynesen, J. & Nielsen, J. (2003). Branching is coordinated with mitosis in growing hyphae of *Aspergillus nidulans*. *Fungal Gen Biol* **40**, 15–24.

Firtel, M. & Beveridge, T. J. (1995). Scanning probe microscopy in microbiology. *Micron* **26**, 347–362.

Gebeshuber, I. C., Kindt, J. H., Thompson, J. B., Del Amo, Y., Stachelberger, H., Brzezinski, M. A., Stucky, G. D., Morse, D. E. & Hansma, P. K. (2003). Atomic force microscopy study of living diatoms in ambient conditions. *J Microsc* **212**, 292–299.

Gebeshuber, I. C., Kindt, J. H., Thompson, J. B., Del Amo, Y., Stachelberger, H., Brzezinski, M. A., Stucky, G. D., Morse, D. E. & Hansma, P. K. (2004). Erratum for: Atomic force microscopy study of living diatoms in ambient conditions. (*J Microsc* **212**, 292–299). *J Microsc* **214**, 101.

Gierz, G. & Bartnicki-García, S. (2000). A three-dimensional model of fungal morphogenesis based on the vesicle supply center concept. *J Theor Biol* **208**, 151–164.

Gooday, G. W. (1994). Cell walls. In *The Growing Fungus*, pp. 43–62. Edited by N. A. R. Gow & G. M. Gadd. London: Chapman & Hall.

Guest, G. M. & Momany, M. (2000). Analysis of cell wall sugars in the pathogen *Aspergillus fumigatus* and the saprophyte *Aspergillus nidulans*. *Mycologia* **92**, 1047–1050.

Harold, F. M. (2002). Force and compliance: rethinking morphogenesis in walled cells. *Fungal Genet Biol* **37**, 271–282.

Heath, I. B. (1990). The roles of actin in tip growth of fungi. *Int Rev Cytol* **123**, 95–127.

Howard, R. J. & O'Donnell, K. L. (1987). Freeze substitution of fungi for cytological analysis. *Exper Mycol* **11**, 250–269.

Jackson, S. L. & Heath, I. B. (1990). Evidence that actin reinforces the extensible hyphal apex of the oomycete *Saprolegnia ferax*. *Protoplasma* **157**, 144–153.

Kaminskyj, S. G. W. (2001). Fundamentals of growth, storage, genetics and microscopy in *Aspergillus nidulans*. *Fungal Genetics Newsletter* **48**, 25–31.

Kaminskyj, S. G. W. & Boire, M. R. (2004). Ultrastructure of the *Aspergillus nidulans hypA1* restrictive phenotype shows defects in endomembrane arrays and polarized wall deposition. *Can J Bot* **82**, 807–814.

Kaminskyj, S. G. W. & Hamer, J. E. (1998). *hyp* loci control cell pattern formation in the vegetative mycelium of *Aspergillus nidulans*. *Genetics* **148**, 669–680.

Kaminskyj, S. G. W. & Heath, I. B. (1995). Integrin and spectrin homologues, and cytoplasm-wall adhesion in tip growth. *J Cell Sci* **108**, 849–856.

Landau, L. D. & Lifshitz, E. M. (1959). *Theory of Elasticity*. London: Pergamon.

Lipke, P. N. & Ovalle, R. (1998). Cell wall ultrastructure in yeast: new structure and new challenges. *J Bacteriol* **180**, 3735–3740.

Mathur, J. & Hulskamp, M. (2002). Microtubules and microfilaments in cell morphogenesis in higher plants. *Curr Biol* **12**, R669–R676.

Meyer, R., Parish, R. W. & Hohl, H. R. (1976). Hyphal tip growth in *Phytophthora*. Gradient distribution and ultrahistochemistry of enzymes. *Arch Microbiol* **110**, 215–224.

Momany, M. (2002). Polarity in filamentous fungi: establishment, maintenance and new axes. *Curr Opin Microbiol* **5**, 580–585.

Momany, M., Lindsey, R., Hill, T. W. & 7 other authors (2004). The *Aspergillus fumigatus* cell wall is organized in domains that are remodelled during polarity establishment. *Microbiology* **150**, 3261–3268.

Money, N. P. & Harold, F. M. (1992). Extension growth in the water mold *Achlya*: interplay of turgor and wall strength. *Proc Natl Acad Sci U S A* **89**, 4245–4249.

Money, N. P. & Hill, T. W. (1997). Correlation between endoglucanase secretion and cell wall strength in oomycete hyphae: implications for growth and morphogenesis. *Mycologia* **89**, 777–785.

Ricci, D. & Grattarola, M. (1994). Scanning force microscopy on live cultured cells: imaging and force-versus-distance investigations. *J Microsc* **176**, 254–261.

Schneider, S. W., Sritharan, K. C., Geibel, J. P., Oberleithner, H. & Jena, B. P. (1997). Surface dynamics in living acinar cells imaged by atomic force microscopy: identification of plasma membrane structures involved in exocytosis. *Proc Natl Acad Sci U S A* **94**, 316–321.

Shi, X., Sha, Y. & Kaminskyj, S. G. W. (2004). *Aspergillus nidulans hypA* regulates morphogenesis through the secretion pathway. *Fungal Gen Biol* **41**, 75–88.

Sietsma, J. H. & Wessels, J. G. H. (1979). Evidence for covalent linkages between chitin and β-glucan in a fungal wall. *J Gen Microbiol* **114**, 99–108.

Sietsma, J. H. & Wessels, J. G. H. (1981). Solubility of (1→3)-β-D (1→6)-β-D-glucan in fungal walls: importance of presumed linkage between glucan and chitin. *J Gen Microbiol* **125**, 209–212.

Small, J. V. & Kaverina, I. (2002). Microtubules meet substrate adhesions to arrange cell polarity. *Curr Opin Cell Biol* **5**, 580–585.

Stokke, B. T., Falch, B. H. & Dentini, M. (2001). Macromolecular triplex zipping observed in derivatives of fungal (1→3)-β-D-glucan by electron and atomic force microscopy. *Biopolymers* **58**, 535–547.

Stringer, M. A., Dean, R. A., Sewall, T. C. & Timberlake, W. E. (1991). *Rodletless*, a new *Aspergillus* developmental mutant induced by directed gene inactivation. *Genes Dev* **5**, 1161–1171.

Torralba, S. & Heath, I. B. (2001). Cytoskeletal and Ca^{2+} regulation of hyphal tip growth and initiation. *Curr Top Dev Biol* **51**, 135–187.

Touhami, A., Nysten, B. & Dufrêne, Y. F. (2003). Nanoscale mapping of the elasticity of microbial cells by atomic force microscopy. *Langmuir* **19**, 4539–4543.

van der Mei, H. C., Busscher, H. J., Bos, R., de Vries, J., Boonaert, C. J. P. & Dufrêne, Y. F. (2000). Direct probing by atomic force microscopy of the cell surface softness of a fibrillated and nonfibrillated oral streptococcal strain. *Biophys J* **78**, 2668–2674.

Vermeulen, C. A. & Wessels, J. G. H. (1984). Ultrastructural differences between wall apices of growing and non-growing hyphae of *Schizophyllum commune*. *Protoplasma* **120**, 123–131.

Vermeulen, C. A. & Wessels, J. G. H. (1986). Chitin biosynthesis by a fungal membrane preparation: evidence for a transient non-crystalline state of chitin. *Eur J Biochem* **158**, 411–415.

Wedlich-Soldner, R. & Li, R. (2003). Spontaneous cell polarization: undermining determinism. *Nat Cell Biol* **5**, 267–270.

Wessels, J. G. (1999). Fungi in their own right. *Fungal Genet Biol* **27**, 134–145.

Xu, X. & Arnsdorf, M. F. (1994). Calibration of the scanning (atomic) force microscope with gold particles. *J Microsc* **173**, 199–210.

Yang, Z. (1998). Signaling tip growth in plants. *Curr Opin Plant Biol* **1**, 525–585.

Yang, J. & Shao, Z. (1995). Recent advances in biological atomic force microscopy. *Micron* **26**, 35–49.

Yao, X., Jericho, M., Pink, D. & Beveridge, T. (1999). Thickness and elasticity of Gram-negative murein sacculi measured by atomic force microscopy. *J Bacteriol* **181**, 6865–6875.

Zhao, L., Schaefer, D., Haixin, X., Modi, S. J., LaCourse, W. R. & Martin, R. (2005). Elastic properties of the cell wall of *Aspergillus nidulans* studied with atomic force microscopy. *Biotechnol Prog* **21**, 292–299.